Magnetic properties of F- and P-type icosahedral quasicrystals of Al - Pd - Mn

1997 J. Phys.: Condens. Matter 9 3205

(http://iopscience.iop.org/0953-8984/9/15/012)

J. Phys.: Condens. Matter **9** (1997) 3205–3217. Printed in the UK PII: S0953-8984(97)78263-8

Magnetic properties of F- and P-type icosahedral quasicrystals of Al–Pd–Mn

Atsushi Kobayashi†, Susumu Matsuo‡, Tsutomu Ishimasa§ and Hiroshi Nakano‡

† Department of Applied Physics, School of Engineering, Nagoya University, Nagoya 464-01, Japan

‡ Department of Natural Science Informatics, School of Informatics and Sciences, Nagoya University, Nagoya 464-01, Japan

§ Department of Nuclear Engineering, School of Engineering, Nagoya University, Nagoya 464-01, Japan

Received 1 October 1996, in final form 20 December 1996

Abstract. The magnetization of F- and P-type icosahedral Al–Pd–Mn was studied in the temperature region between 2 and 870 K in a magnetic field below 80 kOe. F-type icosahedral phase samples obtained by quenching from 1075 K were transformed to the low-temperature-phase form during the magnetic measurement above 600 K. The low-temperature phase is a P-type phase; this phase is characterized by a superlattice ordering. The samples showed Curie–Weiss paramagnetism and increasing susceptibility with increasing temperature at high temperatures. The increasing susceptibility is accounted for by a temperature dependence of the Pauli paramagnetism arising from a pseudogap at E_F in the electronic density of states. The increase in the P phase was larger than that in the F phase, which indicates an enhanced pseudogap in the P phase. This is consistent with a structural transformation to a more stable P phase caused by the *in situ* heat treatment. The Curie–Weiss susceptibility decreased after the structural transformation from F- to P-type structure had occurred. A reduction by about one half in the number of magnetic Mn atoms in the transformation is inferred. The temperature dependence of the susceptibility deviates from the Curie–Weiss law below 30 K, which is similar to what was found in a previous report by Chernikov and co-workers, but the deviation is much smaller.

1. Introduction

Icosahedral quasicrystals were originally found in a rapidly quenched Al–Mn alloy which exhibited an icosahedral symmetry in electron diffraction patterns, which is not allowed for the well-known crystals with periodic translational symmetry [1]. At first the quasicrystals were considered to be realized as metastable phases, but successive intensive studies revealed that the quasicrystals contain various stable phases [2–4]. The phase transformation between the icosahedral phase and the crystal was studied in detail by means of neutron diffraction [5]. Several icosahedral alloys could be made to form single grains of millimetre size or greater, and the physical properties were studied experimentally [6–13]. The icosahedral phases are now known to consist of two types of structure, P type and F type [14]. Dodecagonal [15] and decagonal [16] quasicrystals were discovered subsequently; these had an orientational symmetry inconsistent with periodic symmetry in a plane. Therefore the quasicrystals now occupy the position of a new class of material with a new class of

0953-8984/97/153205+13$19.50

symmetries which includes a rich variety of alloys, for which, however, several problems have not been fully resolved yet: (i) the atomic occupation has not been definitely determined for the icosahedral quasicrystals in spite of elaborate studies [17–19] as yet, (ii) the electrical conductivity of some of the icosahedral phases is extremely small, corresponding to a very short mean free path comparable to the interatomic distance [13, 20] or suggesting a quantum interference effect in the insulating regime [21, 22], (iii) only a very small proportion of the Mn atoms are magnetic in the icosahedral phase containing Mn [23–25], and (iv) a curious behaviour was observed in the Curie–Weiss susceptibility of the Al–Pd–Mn icosahedral phase, with two different Curie constants and Curie temperatures in two different temperature regions [26].

The rich variety of the new class of material was further augmented by a recent discovery of superlattice ordering in Al–Pd–Mn alloys, in which a high-temperature F-type icosahedral phase transformed to a P-type phase below approximately 600 °C in a narrow range of composition near $Al_{71.0}Pd_{21.0}Mn_{8.0}$ [27]. This P-type phase has different structure to the original P-type Al–Mn phase [1], and is characterized by the appearance of weak superlattice reflections at the centre of two fundamental reflections. Here 'fundamental reflections' means the reflections observed also in the high-temperature F-type phase. The P-type phase has an approximately τ times larger six-dimensional lattice parameter as compared with the F-type phase, where τ denotes the golden mean. The difference between the electronic properties of the two icosahedral phases is interesting in relation to the origin of the two different structures, because the stability of an icosahedral Al–Pd–Mn quasicrystal was thought to have an electronic origin [28].

The electronic origin of the stability of the quasicrystals has been studied theoretically [29–31] and experimentally [28, 32–37] on the basis of the valley-like structure (pseudogap) at E_F in the electronic density of states (DOS), which is mainly related to the strong-diffraction spots. The valley-like structure can be investigated experimentally via the UPS study of the DOS [36], the electronic specific heat coefficient [34, 35], or the temperature dependence of the Pauli paramagnetism [32, 33, 37, 38]. The UPS study is the most direct method, but is not easy to conduct at high temperatures. The temperature dependence of the Pauli paramagnetism gives the curvature of the DOS at E_F, and affords a simple *in situ* measurement [37] at high temperatures, which is most suitable for the study of the possible structural transformation between the two icosahedral phases [27]. Magnetic measurement at low temperatures gives further information about the local magnetic moments. The formation of magnetic moments of Mn was suggested to be governed by a delicate condition dependent on the local environment of the Mn atoms [24].

Icosahedral $Al_{71.0}Pd_{20.5}Mn_{8.5}$ and $Al_{71.0}Pd_{21.0}Mn_{8.0}$ samples were prepared in the present study in order to clarify the DOS at E_F, the properties of the local magnetic moments, and the Curie–Weiss paramagnetism at low and high temperatures of the F and P icosahedral phases.

2. Experimental procedure

Materials of nominal compositions 71.0 at.% Al–20.5 at.% Pd–8.5 at.% Mn (sample 1) and 71.0 at.% Al–21.0 at.% Pd–8.0 at.% Mn (sample 2) were melted in a plasma jet furnace. The purities of the starting materials were 99.999%, 99.95%, and 99.95% for Al, Pd, and Mn, respectively. They were put into graphite crucibles, and sealed in vacuum in quartz tubes. They were annealed at 802 °C for 18 hours, and quenched into water. The resulting ingots were F-type icosahedral phases. The electron diffraction pattern of sample 1 is shown in figure 1(a).

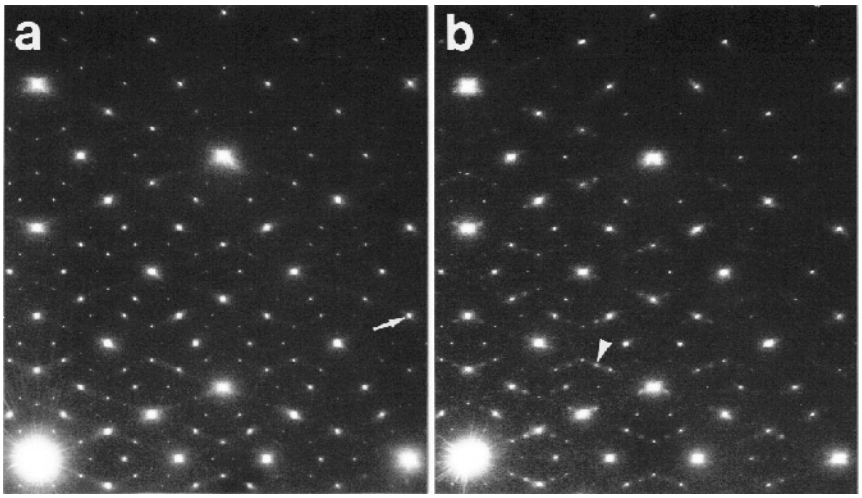

Figure 1. (a) The electron diffraction pattern of sample 1 in the F-type icosahedral phase, and (b) that of the P-type icosahedral phase, after structural transformation. The direction of the threefold axis is indicated by an arrow in (a). An example of superlattice reflection characteristic of the P structure is shown by an arrow-head in (b).

All of the observed diffraction spots could be indexed to the F-type icosahedral quasilattice. The strong diffuse intensity observed along the directions of the threefold axis is the indication of structural disorder in this quenched F-type phase. Such a threefold streak is related to the occurrence of the superlattice ordering at low temperature. The composition of the ingot of sample 1 was analysed by means of energy-dispersive x-ray microanalysis using a JEOL JEM5400/QX2000 scanning microscope. The composition found by analysis was $Al_{67}Pd_{22}Mn_{10}$. The discrepancy between the composition found by analysis and the nominal one was within the experimental error of this analysis.

The samples were taken out from the crucibles, the surfaces in contact with the graphite were removed using emery papers, and the samples were rinsed in acetone using an ultrasonic washing apparatus. They were sealed in quartz cells in a He atmosphere of 0.3 atm pressure to ensure thermal equilibrium with the magnetization measurement apparatus.

The magnetic force of the sample and the quartz cell was measured by the use of Faraday-type magnetic balances. The balance used below 256 K was equipped with two superconducting magnets, one of which produced the main magnetic field below 80 kOe while the other produced the gradient field of 1128 Oe cm^{-1}. The sensitivity of the electrobalance was 1×10^{-7} cgs emu for the magnetic moment. The balance used above 256 K was equipped with a standard electromagnet producing the main magnetic field of 10 kOe, and the magnetic field gradient of the main field was utilized. The sensitivity was 1×10^{-6} cgs emu for the magnetic moment. The magnetization was linearly dependent on the magnetic field above 256 K, and the susceptibility measurement was made at 10 kOe above that temperature. The magnetic susceptibility χ was determined in the linear region of the field dependence of the magnetization over the whole temperature region.

The quartz cells were cracked to remove the samples from them after the measurement was completed, and then put together again using glass adhesive to restore the shape. Then the magnetic force of the cells only was measured. The force was independent of the temperature above 16 K, and slightly dependent on temperature below that temperature. The force of the cells was subtracted from that of the samples and the cells to give the net

magnetization of the samples.

The magnetization of the initial F-type samples was measured in the temperature region between 2 and 256 K with the magnetic balance equipped with the superconducting magnet, and then it was measured above 77 K with the balance equipped with the standard electromagnet. The sample structure transformed to P-type icosahedral structure in the high-temperature measurement. The magnetization of the P-type samples was measured in the temperature region between 2 and 873 K.

The electron diffraction pattern of sample 1 after the structural transformation is shown in figure 1(b). An example of the superlattice reflections characteristic of the P-type phase is shown by the arrow-head. All of the weak reflections located at the centre of the two fundamental reflections could be interpreted in terms of the superlattice ordering. These superlattice reflections had broader shapes than the fundamental reflections. In the powder x-ray diffraction experiment, it was quite difficult to recognize the superlattice reflections, because of the very weak intensity of the superlattice reflections, and because of the trace of an unidentified crystal phase especially in sample 1. However, the intensity of the strongest x-ray diffraction peak of the impurity crystal was less than 0.8% of that of the strongest icosahedral peak. The structural transformation of sample 2 was not complete, in view of the electron microscope observation which indicated traces of a portion that had still not been transformed after the high-temperature magnetic balance measurement. The volume of the part that had not been transformed was deduced to be about one third of the sample, from the results of the electron microscope observation. Therefore discussions on the change in the magnetization of sample 2 should be taken as semiquantitative.

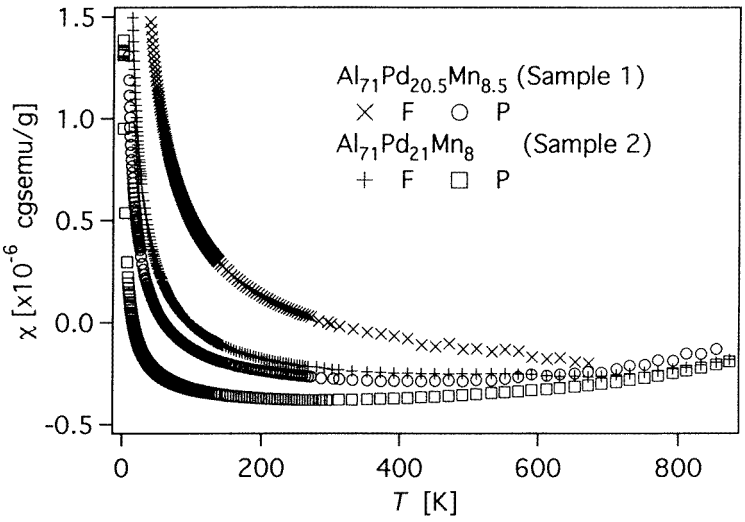

Figure 2. The temperature dependence of the magnetic susceptibility χ for samples 1 and 2 before the high-temperature measurements (F type) and after them (P type).

3. Results and discussion

The temperature dependence of the magnetic susceptibility χ for samples 1 and 2 is shown in figure 2 before the high-temperature measurements (F type) and after them (P type).

The characteristics of the magnetism are qualitatively summarized as follows. All of the samples show Curie–Weiss (C–W) paramagnetism at low temperatures. The C–W paramagnetism is reduced in P-type samples as compared with the corresponding F-type ones. The susceptibility χ at high temperatures increases with the rise in temperature except for sample 1 in its F-phase form. These characteristics are quantitatively analysed in the following.

3.1. The temperature dependence of the susceptibility

A least-squares fitting of χ to the Curie–Weiss law

$$\chi = \chi_0 + C/(T - \Theta) \tag{1}$$

was tried for sample 1, where χ_0 denotes a term independent of temperature, C is the Curie constant, and Θ is the Curie temperature. The temperature region of the data for the fitting was selected so that the parameters obtained from the fit did not change with the width of the selected region within the error of the parameters arising from the scattering of the data. The temperature regions adopted were between 100 and 270 K for the F phase and between 50 and 150 K for the P phase. The results of the fit are shown in figures 3(a) and 3(b). The temperature was raised by 20 K at twenty-minute intervals above 400 K. The magnetic susceptibility was checked as remaining unchanged after being additionally held at 500 K for 100 min, and the diffraction was checked as showing the F-type pattern. This means that the transformation to the P phase does not occur below that temperature. The data for the F phase are in good agreement with the fitting curve below 500 K, but deviate slightly downward above 600 K. The deviation in the susceptibility was observed as an irreversible change resulting from the annealing in the high-temperature measurement.

The irreversible deviation might be suspected to originate from Mn vaporization in the annealing. However, the inner wall of the sample capsule showed little change in colour. Furthermore, another sample taken from the same ingot was again water quenched from 800 °C for 18 hours after the *in situ* annealing in the high-temperature measurement in order to check the recovery of the susceptibility. The susceptibility showed nearly the same value as that after the first water quench: within 6%. Therefore the Mn vaporization effect can be neglected. Another possible explanation for the deviation in the susceptibility is the Mn migration from the icosahedral phase to the impurity crystal phase, because varying the Mn content from 8.5 to 8.0% can change the Curie constant by a factor of 3 [25]. However, such a change in the main icosahedral phase would imply the unlikely situation of the impurity phase less than 0.8% consisting almost entirely of Mn. Therefore the irreversible deviation is most probably to be considered as corresponding to the precursor of the structural transformation to the more stable P phase. Sample 1 was then annealed in the magnetic balance at 773 K for 18 hours to complete the transformation to the P phase.

The result of the Curie–Weiss fit is shown for sample 1 after the transformation to the P phase by a dotted curve in figure 3(b). The data are in good agreement with the fitting curve below 300 K, but deviate upward above it. The deviation was reversible, and therefore the upward increase in χ is inherent in sample 1 in its P-phase form. Such an increase in χ at high temperatures has been observed in the stable icosahedral phases Al–Cu–Fe [32, 33], Ga–Mg–Zn [37], Al–Pd–Mn [28], and Al–Cu–Ru [38]. It was interpreted in terms of the temperature dependence of the Pauli paramagnetism resulting from the valley-like structure at E_F in the DOS [28, 32, 33, 37, 38], which is closely related to the stability of the icosahedral phases.

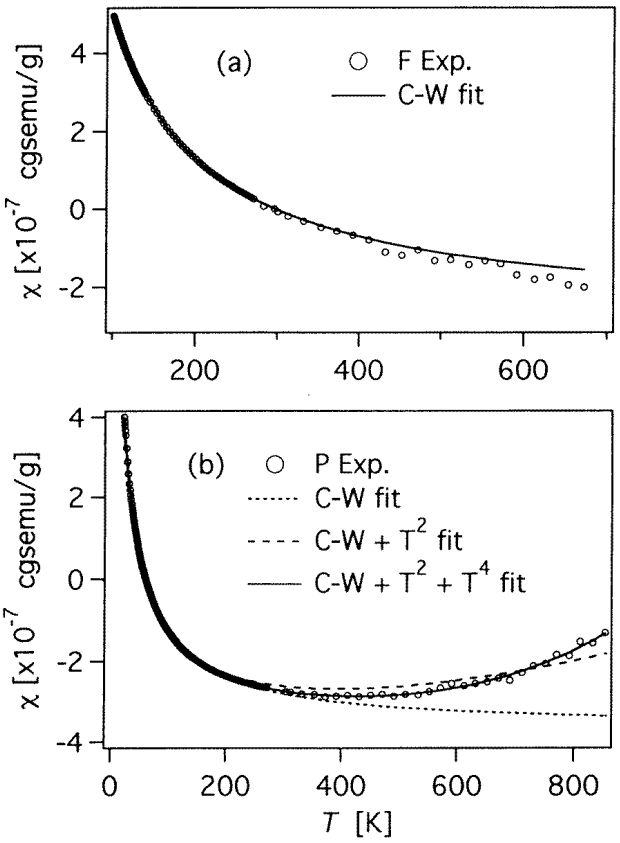

Figure 3. (a) The temperature dependence of the magnetic susceptibility χ of sample 1 ($Al_{71}Pd_{20.5}Mn_{8.5}$) in its F-type form, and the C–W fitting based on equation (1). (b) The temperature dependence of χ of sample 1 in its P-type form, and various fittings based on equations (1), (2), and (4).

Therefore a fitting of χ to the following function was tried for sample 1 in its P-type form. The function consists of a constant susceptibility, the Curie–Weiss term, and the first temperature-dependent correction [39]—proportional to T^2—of the Pauli paramagnetism:

$$\chi = \chi_0 + C/(T - \Theta) + AT^2 \tag{2}$$

where

$$A = \frac{\mu_B^2 N(E_F)(\pi k)^2}{3}\left\{\frac{1}{N(\zeta)}\left(\frac{d^2N(\zeta)}{d\zeta^2}\right) - \left(\frac{1}{N(\zeta)}\frac{dN(\zeta)}{d\zeta}\right)^2\right\}_{\zeta=E_F}. \tag{3}$$

The quantity $N(\zeta)$ denotes the electronic density of states, μ_B the Bohr magneton, and E_F the Fermi energy at 0 K. The result of the fitting is shown by a dashed curve in figure 3(b). The curve indicates an improved agreement with the experimental data, but the agreement is not satisfactory. A similar disagreement can be noticed in the temperature dependence of the Knight shift for the $Al_{65}Cu_{20}Ru_{15}$ icosahedral phase [38]. Therefore a fitting of χ to the following function, which includes the higher-order temperature-dependent correction—

proportional to T^4—of the Pauli paramagnetism, was tried:

$$\chi = \chi_0 + C/(T - \Theta) + AT^2 + BT^4. \tag{4}$$

The coefficient B contains complicated contributions from derivatives of $N(E_F)$ up to fourth order, the explicit form of which is given in the appendix. The result of the fitting for the data above 50 K is shown by the solid curve in figure 3(b). The curve indicates a good agreement with the experimental data. The necessity of the inclusion of the T^4-term means that the separation between the T^2- and T^4-terms is meaningful.

Table 1. Parameters determined from the fitting including constant, Curie–Weiss, T^2-, and T^4-terms (upper half), and from the Curie–Weiss law below 16 K with fixed χ_0 (lower half). See the text for details.

		χ_0 (10^{-7} emu g^{-1})	Θ (K)	C (10^{-5} emu K g^{-1})	P_{eff} (μ_B)	A (10^{-13} emu g^{-1} K^{-2})	B (10^{-19} emu g^{-1} K^{-4})
Sample 1	F	−2.82	−12.1	8.73	0.61	—	—
($Al_{71}Pd_{20.5}Mn_{8.5}$)	P	−3.67	−12.8	2.72	0.34	0.41	3.27
Sample 2	F	−3.64	−10.1	3.88	0.42	0.91	2.21
($Al_{71}Pd_{21}Mn_8$)	P	−4.37	−14.4	1.26	0.24	1.89	1.41
Sample 1 ($\leqslant$16 K)	F	−2.82	−0.76	6.14	0.51		
($Al_{71}Pd_{20.5}Mn_{8.5}$)	P	−3.67	−1.11	1.49	0.25		
Sample 2 ($\leqslant$16 K)	F	−3.64	−1.10	2.67	0.35		
($Al_{71}Pd_{21}Mn_8$)	P	−4.37	−2.44	0.70	0.18		

The parameters χ_0, Θ, C, A, and B obtained by the fitting are shown in the first and second rows in table 1. The parameter values quantitatively indicate the trend inferred from figure 2: that the Curie constant is reduced and the coefficient A becomes positive from zero after sample 1 is transformed from the F to the P phase. The positive value of A indicates that a valley-like structure is formed in the DOS at E_F in the more stable P phase of sample 1, as in the other stable icosahedral phases [32, 33, 37, 38], because the second term in the braces of equation (3) always makes a negative contribution to A. The coefficient B contains complicated contributions from various derivatives, and such a clear conclusion cannot be deduced from it. The reduction in the Curie constant suggests a change in the environment of the Mn sites [24, 40] or in the clustering of Mn atoms [40, 41].

A similar measurement was made on sample 2 with a slightly different composition in order to confirm the above trend in the transformation from the F to the P phase. The long-time annealing in the magnetic balance was made at 873 K for 48 hours. The same trend in the difference between the F and the P phases as shown in figure 2 is evident for sample 2. The least-squares-fitting curves based on equation (4) are shown in figures 4(a) and 4(b), and are in good agreement with the experimental data. The parameter values obtained from the fit are shown in the third and fourth rows in table 1. The increase in the coefficient A after the structural transformation is same as for sample 1, although it is perhaps only fair to note that this argument depends on the separation of the T^2- and T^4-terms in sample 2, because of the existence of a T^4-term in both the F and P phases.

A considerable decrease was observed in the Curie constant in the transformation from the F to the P phase for both samples. The Curie constant is a composite of the following quantities: the angular momentum J, the g-factor, and the density of local magnetic moments. More detailed information about the local magnetic moments is obtained from the following analysis of the magnetic field dependence of the magnetization.

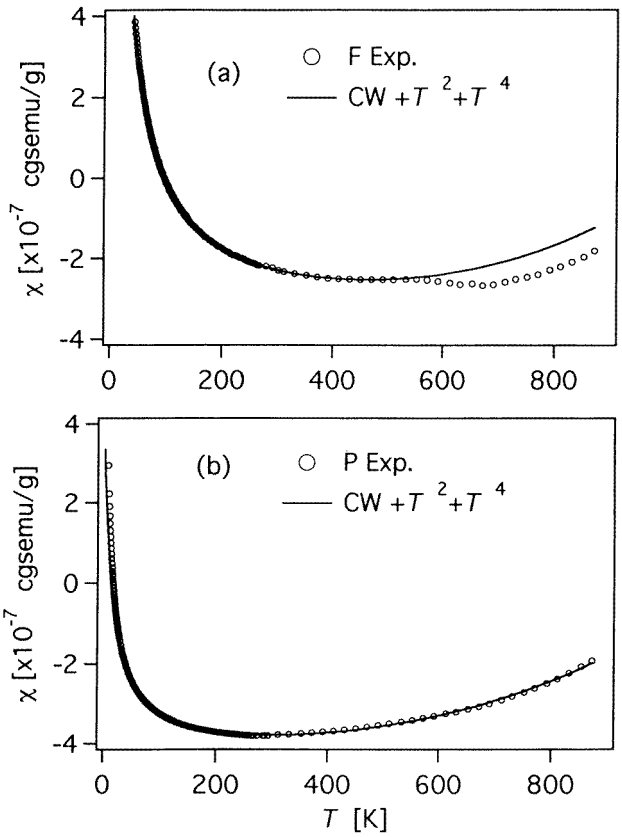

Figure 4. (a) The temperature dependence of the magnetic susceptibility χ of sample 2 ($Al_{71}Pd_{21}Mn_8$) in its F-type form, and the fitting based on equation (4). (b) The temperature dependence of χ of sample 2 in its P-type form, and the fitting based on equation (4).

3.2. The magnetic field dependence of the magnetization

The magnetization σ is shown as a function of the magnetic field H for the F and P phases of sample 1, $Al_{71}Pd_{20.5}Mn_{8.5}$, in figures 5(a) and 5(b), respectively. The figures clearly show the decrease in the paramagnetism of the local magnetic moments with the transformation from the F to the P phase. The magnetization of $Al_{71}Pd_{21}Mn_8$ showed a similar trend in the structural transformation. Fitting to a Brillouin function [28] may be appropriate for investigating the properties of the local magnetic moments with due regard given to a constant diamagnetic contribution in view of the trend towards saturation at low temperatures, and the negative slope at high temperatures in figure 5.

The $\sigma - \chi_0 H$ versus H/T data for sample 2 in its P-type form were fitted to a Brillouin function, where χ_0 was determined from the fit of the temperature dependence of χ to equation (4) (table 1). The fitted curves are in good agreement with the experimental data except at the lowest temperatures. The parameter values obtained are almost independent of temperature at 12, 14, and 16 K. The differences between the values are within 10%. The antiferromagnetic coupling indicated in the negative Curie temperature (the second column in table 1) is considered to cause the disagreement between the data and the fitted curves at

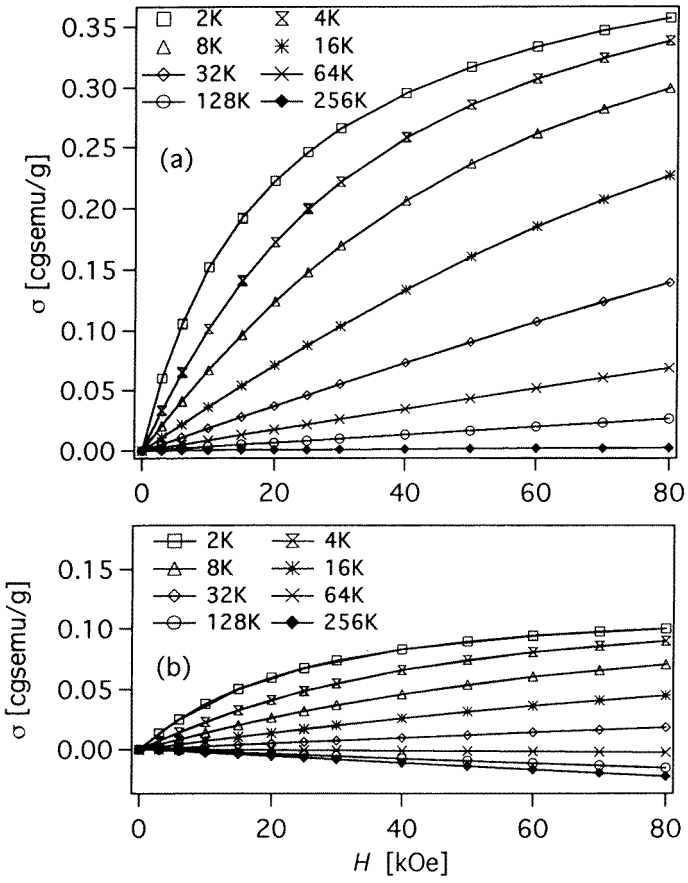

Figure 5. (a) Magnetization as a function of magnetic field for sample 1 ($Al_{71}Pd_{20.5}Mn_{8.5}$) in its F-type form. (b) Magnetization as a function of magnetic field for sample 1 in its P-type form. The curves are only given as a guide for the eyes.

the lowest temperatures. Therefore it is reasonable to adopt the parameter values obtained at 16 K as a good approximation, because the effect of the antiferromagnetic coupling becomes less important at higher temperatures on account of the thermal agitation.

Table 2. Parameters determined from the Brillouin fit at 16 K. N denotes the number of local moments per gram, g the g-factor, and J the angular momentum. The χ_0-values in table 1 were used in the fitting of $\sigma - \chi_0 H$.

	Sample 1 ($Al_{71}Pd_{20.5}Mn_{8.5}$)		Sample 2 ($Al_{71}Pd_{21}Mn_8$)	
	F	P	F	P
$N(10^{18}\ g^{-1})$	7.22	2.94	4.98	2.92
g	1.86	1.71	1.88	1.95
J	2.87	2.30	2.18	1.18

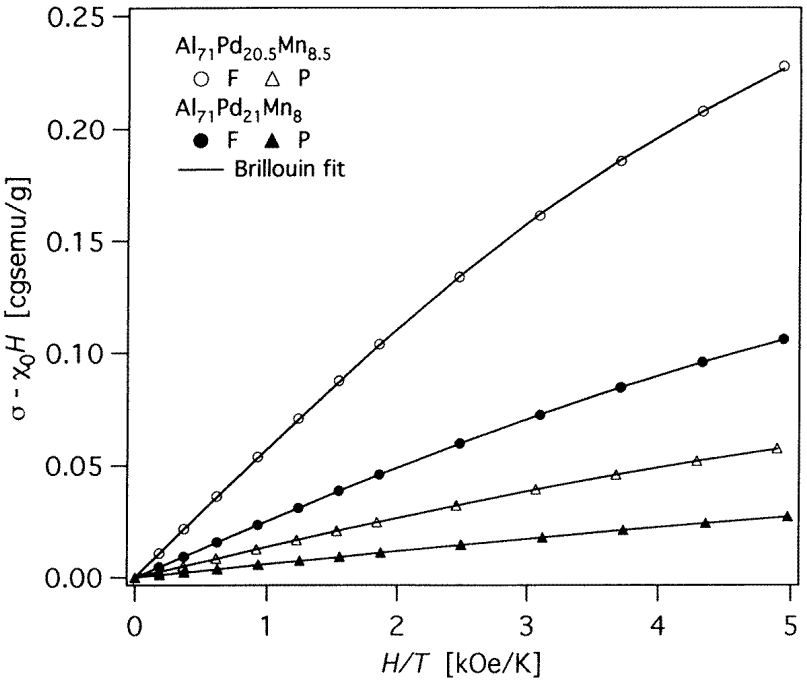

Figure 6. $\sigma - \chi_0 H$ as a function of H/T for samples 1 and 2 at 16 K. The χ_0-values from table 1 were used.

Figure 6 shows curves fitted to the Brillouin function and the data for the F and P phases of $Al_{71}Pd_{20.5}Mn_{8.5}$ and $Al_{71}Pd_{21}Mn_8$ at 16 K. The agreement with the data is excellent. Table 2 shows the parameter values obtained from the fit. The g-factor is nearly 2, which indicates that the local moments mainly originate from spin angular momentum. The orbital angular momentum may be quenched in the local low symmetry in the icosahedral quasilattice.

A remarkable feature common to the two samples (table 2) is a decrease in the number of local magnetic moments N after the transformation from the F to the P phase. The decrease may be accounted for by a reduction in the number of magnetic Mn atoms caused by a change in the environment of the Mn sites [24, 40] or in the clustering of Mn atoms [40, 41]. The angular momentum J between about 5/2 and 2/2 (the third row in table 2) may be attributed to one Mn atom or to a cluster of antiferromagnetically coupled Mn atoms [26]. The decrease in the Curie constant C discussed in section 3.1 is consistent with the reduction in the number of magnetic Mn atoms, because the temperature region adopted for the fit is much higher than the antiferromagnetic Curie temperatures shown in table 1, and the individual Mn moments must thermally fluctuate independently to give the Curie constant arising from individual Mn moments. Therefore the decrease in N is most probably accounted for by the reduction in the number of magnetic Mn atoms which may result from a change in the environment of the Mn sites [24, 40] including the possibility of a change in the distance between the Mn atoms [41]. Structural models of the transformation to be investigated must be consistent with the present change in N. The number of magnetic Mn atoms is about 1% and 0.5% of the total number of Mn atoms for the F and P samples, respectively.

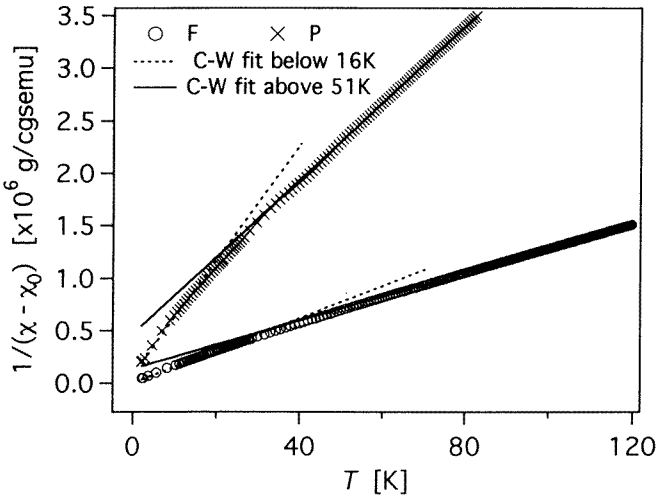

Figure 7. The inverse of the susceptibility χ excluding the constant χ_0 as a function of the temperature for the F and P phases of sample 1, where the χ_0-values from table 1 were used. The solid line shows the Curie–Weiss law for the higher-temperature fit in table 1. The broken line shows the Curie–Weiss fit below 16 K.

3.3. Curie–Weiss paramagnetism at low temperatures

Figure 7 shows the inverse of the susceptibility χ of sample 1, with the constant term χ_0 excluded, as a function of temperature below 120 K for the F and P phases. The figure indicates that the temperature dependence of χ deviates below about 20–30 K from the Curie–Weiss law determined at high temperatures. Sample 2 showed the same trend. The feature can also be seen in figure 4(b). The data below 16 K can again be fitted to equation (1), and parameters obtained from the fit are shown in table 1. The table indicates that the Curie temperature Θ and the effective magnetic moment P_{eff} decrease at low temperatures.

The above feature is qualitatively similar to a previous report [26]. It was interpreted on the basis of antiferromagnetic clustering or a strongly frustrated spin-glass model [26]. The absolute value of Θ obtained from the fit at higher temperature is much smaller than the previously reported value, $|-108|$ K [26]. The reason for the difference between the present result and the previous one is not clear. On the assumption of a clustering mechanism, the difference might be concerned with the difference in the sample homogeneity. On adopting a strongly frustrated spin-glass model, the difference might correspond to the difference in the frustration, the details of which are not, however, known.

4. Conclusion

An increase in χ was observed at high temperatures, and was interpreted on the basis of a temperature dependence of the Pauli paramagnetism arising from the valley-like structure at E_F in the DOS. The coefficient of the T^2-term was larger in the P phase than in the F phase, which strongly suggests an enhanced valley-like structure in the P phase. This is consistent with a structural transformation to the more stable P phase via the annealing. The Curie–Weiss susceptibility of the P-type samples was about one third of that of the corresponding F-type samples. This corresponds to there being fewer magnetic Mn atoms in the P phase

than in the F phase, which is also inferred from the magnetization versus magnetic field curves at low temperatures. Two different Curie constants and Curie temperatures were observed in two different temperature regions, but the difference was much smaller than the previously reported one [26].

Acknowledgments

The authors would like to thank Mr E Takeuchi and Mr Y Hayashi for assembling the magnetic balances for the measurements at low and high temperatures.

Appendix

The correction term of the Pauli paramagnetism of the order of T^4 is calculated by the use of equations (6.4.3), (6.4.4) and (A4.6) of reference [39], where proper consideration [38] has to be given to the temperature dependence of the chemical potential ζ. The result is

$$B = 2\mu_B^2 N(E_F)k^4 \left\{ -\frac{\pi^4}{72}\frac{1}{N(\zeta)^4}\left(\frac{dN(\zeta)}{d\zeta}\right)^4 + \frac{3\pi^4}{72}\frac{1}{N(\zeta)^3}\left(\frac{dN(\zeta)}{d\zeta}\right)^2\left(\frac{d^2N(\zeta)}{d\zeta^2}\right) - \frac{17\pi^4}{360}\frac{1}{N(\zeta)^2}\left(\frac{dN(\zeta)}{d\zeta}\right)\left(\frac{d^3N(\zeta)}{d\zeta^3}\right) + \frac{7\pi^4}{360}\frac{1}{N(\zeta)}\left(\frac{d^4N(\zeta)}{d\zeta^4}\right)\right\}_{\zeta=E_F}.$$

References

[1] Shechtmann D, Blech I, Gratias D and Cahn J W 1984 *Phys. Rev. Lett.* **53** 1951
[2] Dubost B, Lang J M, Tanaka M, Sainfort P and Audier M 1986 *Nature* **324** 48
[3] Tsai A P, Inoue A and Masumoto T 1987 *Japan. J. Appl. Phys.* **26** 1505
[4] Tsai A P, Inoue A, Yokoyama Y and Masumoto T 1990 *Mater. Trans. Japan Inst. Met.* **31** 98
[5] Dubois J M, Dong C, Janot C, de Boissieu M and Audier M 1991 *Phase Transitions* B **32** 3
[6] Kimura K, Iwahasi H, Hashimoto T, Takeuchi S, Mizutani U, Ohashi S and Itoh G 1989 *J. Phys. Soc. Japan* **58** 2472
[7] Shibuya T, Hashimoto T and Takeuchi S 1990 *J. Phys. Soc. Japan* **59** 1917
[8] Zhang Dian-lin, Lu Li, Wang Xue-mei, Lin Shu-yuan, He L X and Kuo K H 1990 *Phys. Rev.* B **41** 8557
[9] Ishimasa T and Mori M 1990 *Phil. Mag. Lett.* **62** 357
[10] Goldman A I, Stassis C, Bellisent R, Moudden H, Pyka N and Gayle F W 1991 *Phys. Rev.* B **43** 8763
[11] Yokoyama Y, Tsai A P, Inoue A and Masumoto T 1991 *Mater. Trans. Japan Inst. Met.* **32** 1089
[12] Matsuo S, Ishimasa T, Mori M and Nakano H 1992 *J. Phys.: Condens. Matter* **4** 10 053
[13] Matsuo S and Nakano H 1992 *Solid State Commun.* **84** 947
[14] Levitov L S and Rhyner J 1988 *J. Physique* **49** 1835
[15] Ishimasa T, Nissen H-U and Fukano Y 1985 *Phys. Rev. Lett.* **55** 511
[16] Bendersky L 1985 *Phys. Rev. Lett.* **55** 1461
[17] Janot C and Mosseri R (ed) 1995 *Proc. 5th Conf. of Quasicrystals* (Singapore: World Scientific)
[18] Boudart M, de Boissieu M, Janot C, Heeger G, Beeli C, Nissen H-U, Vincent H, Ibberson R, Audier M and Dubois J M 1992 *J. Phys.: Condens. Matter* **4** 10 149
[19] Cornier-Quiquandon M, Quivy A, Lefebvre S, Elkaim E, Heeger G, Katz A and Gratias D 1991 *Phys. Rev.* B **44** 2071
[20] Sahnoune A, Ström-Olsen J O and Zaluska A 1992 *Phys. Rev.* B **46** 10 629
[21] Pierce F S, Guo Q and Poon S J 1994 *Phys. Rev. Lett.* **73** 2220
[22] Poon S J, Pierce F S and Guo Q 1995 *Phys. Rev.* B **51** 2777
[23] Stadnik Z M and Stroink G 1991 *Phys. Rev.* B **43** 894
[24] Matsuo S, Nakano H, Ishimasa T and Mori M 1993 *J. Phys. Soc. Japan* **62** 4044
[25] Lasjaunias J C, Sulpice A, Keller N, Prejean J J and de Boissieu M 1995 *Phys. Rev.* B **52** 886
[26] Chernikov M A, Bernasconi A, Beeli C, Schilling A and Ott H R 1993 *Phys. Rev.* B **48** 3058

[27] Ishimasa T 1995 *Proc. 5th Int. Conf. on Quasicrystals* ed C Janot and R Mosseri (Singapore: World Scientific) p 648
[28] Saito K, Matsuo S, Nakano H, Ishimasa T and Mori M 1994 *J. Phys. Soc. Japan* **63** 1940
[29] Friedel J 1988 *Helv. Phys. Acta* **61** 538
[30] Fujiwara T and Yokokawa T 1990 *Quasicrystals (Springer Series in Solid State Science 93)* (Berlin: Springer) p 196
[31] Hafner J and Krajci M 1990 *Europhys. Lett.* **17** 145
[32] Matsuo S, Ishimasa T, Nakano H and Fukano Y 1988 *J. Phys. F: Met. Phys.* **18** L175
[33] Matsuo S, Ishimasa T, Nakano H and Fukano Y 1989 *J. Phys.: Condens. Matter* **1** 6893
[34] Wagner J L, Wong K M and Poon J 1989 *Phys. Rev.* B **39** 809
[35] Wagner J L, Biggs B D and Poon J 1990 *Phys. Rev. Lett.* **65** 203
[36] Mori M, Matsuo S, Ishimasa T, Matsuura T, Kamiya K, Inokuchi H and Matsukawa T 1991 *J. Phys.: Condens. Matter* **3** 767
[37] Saito K, Matsuo S and Ishimasa T 1993 *J. Phys. Soc. Japan* **62** 604
[38] Hill E A, Chang T C, Wu Y, Poon S J and Stadnik Z M 1994 *Phys. Rev.* B **49** 8615
A contribution from the temperature dependence of the chemical potential seems to be missing in equation (7). Proper consideration of the temperature dependence gives derivatives of the DOS in the coefficient of T^3 similar to the corresponding derivatives in the coefficient of T^2 in equation (4).
[39] Wilson A H 1965 *The Theory of Metals* (London: Cambridge University Press) p 151
Wilson A H 1965 *The Theory of Metals* (London: Cambridge University Press) p 331
[40] Stadnik Z M and Stroink G 1989 *Phys. Rev.* B **39** 9797
[41] Chatterjee R, Dunlap R A, Srinivas V and O'Handley R C 1990 *Phys. Rev.* B **42** 2337